J Mater Sci: Mater Med (2010) 21:155–159
DOI 10.1007/s10856-009-3865-3

Synthesis of mesoporous structured hydroxyapatite particles using yeast cells as the template

Wen He · Zhengmao Li · Yingjun Wang · Xiaofeng Chen · Xudong Zhang · Hongshi Zhao · Shunpu Yan · Weijia Zhou

Received: 4 April 2009 / Accepted: 26 August 2009 / Published online: 22 September 2009

Abstract In this study, hydroxyapatite (HAp) particles with mesoporous structure have been synthesized from calcium hydroxide and di-ammonium hydrogen phosphate using yeast cells as the template. The characterization methods such as X-ray diffraction (XRD), Fourier transform infrared spectrograph (FTIR), N_2 adsorption–desorption isotherms (NADI), transmission electron microscopy (TEM) and field emission scanning electron microscopy (FESEM) were used for determination of the particles structure (particle size, structural evolution and morphology). The results show that HAp particles with mesoporous structure could be produced. The size of HAp particles was approximately hundreds of nanometer. The pore width of HAp particles was in the range of 2.0–40 nm and the maximum centered around 4.5 nm.

1 Introduction

Hydroxyapatite, with the structural formula of $Ca_{10}(PO_4)_6(OH)_2$, has a composition and structure very close to natural bone mineral [1–3]. It has been widely considered as one of the most important bioceramics for medical and dental applications such as dental implants and drug delivery systems due to its biocompatibility and bioactivity [1–5]. HAp is used mostly as particles and its application depends on the properties such as particle size, surface area and morphology as well. The mesoporous structure of HAp particles (pore size: 2–50 nm) could be desirable for their use in drug delivery systems. For instance, it could be used as an efficient drug delivery agent to retard the multiplication of cancer cells [6].

There are some methods, which have been developed to prepared the nano-sized HAp particles, involving sol–gels [7, 8], precipitation [9, 10], hydrothermal [11], emulsion [12] and ultrasonic spray freeze-drying [13] methods. To our knowledge, surfactant based template systems have a lot of promise to synthesize fine structured materials, as they are assumed to be efficient template for particle size and shape [14, 15], however, up to now, it is seldom reported that using microbe cells as template to synthesized mesoporous structured HAp particles.

Microbial cells include a wide variety of surface active compounds. They have been receiving increasing attention due to their unique properties, such as higher biodegradability and lower toxicity as well as versatile biological functions compared to chemically synthesized surfactants [16, 17]. All living cells have developed mechanisms by which they take up both essential and non-essential metals, store them, detoxify or dispose them. Initial biosorption of cadmium ions involves both the microbial cells wall and extracellular glycoprotein which are capable of binding heavy metal ions [18].

In this study, the role of microbial cells during the synthesis of HAp particles was examined. The effect of the yeast cells as the template on control of the size and

W. He (✉) · Z. Li · Y. Wang (✉) · X. Chen
Institute of Biomedical Engineering, South China University of Technology, Guangzhou 510640, People's Republic of China
e-mail: hewen1960@126.com

Y. Wang
e-mail: imwangyj@scut.edu.cn

W. He · Z. Li · X. Zhang · S. Yan · W. Zhou
Department of Materials Science and Engineering, Shandong Institute of Light Industry, Jinan 250353, People's Republic of China

H. Zhao
Institute of Crystal Materials, Shandong University, Jinan 250100, People's Republic of China

shape of HAp particles was analyzed. Various characterization techniques were introduced to determine and verify the phase and microstructure presented inside the samples.

2 Experimental

2.1 Materials

The starting materials used in this study included calcium hydroxide ($Ca(OH)_2$, 95%, Sinopharm Chemical Reagent Co., Ltd.), di-ammonium hydrogen phosphate ($(NH_4)_2HPO_4$, 99.0%, Tianjin Baishi Chemical and Industry Ltd.) and yeast cells (Angel Yeast Co., Ltd.). All chemical reagents are in analytical grade. Deionized water was used to make the aqueous solution.

2.2 Synthesis

At room temperature, 0.8 g of active dry yeast cells were cultivated in 40 ml glucose aqueous solution (5 wt%) for 30 min, then 1.56 g of $Ca(OH)_2$ was added into the above solution with stirring for 20 min. To form a reaction mixture, 24 ml of $(NH_4)_2HPO_4$ aqueous solution (0.5 M) was dropwise to the above stirring suspension (pH = 12); stirring was continued for another 30 min. After aging 1 day, the precipitate were separated by centrifugation at 4500 rpm, and then washed twice with deionized water, once with ethanol. Finally, the resultant sample was dried at 80°C for 1 day, and calcined at 700°C for 2 h.

2.3 Characterization procedures

The identification of crystal phases of the obtained products was carried out by X-ray powder diffraction (XRD) technique, using a PANalytical X'Pert PRO X-ray diffractometer (Netherlands) with Cu Kα (λ = 0.15418 nm) incident radiation. Fourier transform infrared spectrograph (FTIR) was performed using a Nicolet Nexus spectrometer (NEXUS 470, Nicolet, USA). The N_2 adsorption–desorption isotherms (NADI) and Barret–Joyner–Halenda (BJH) pore size distribution plot were carried out at 77 K using a computer controlled sorption analyzer (Micromeritics, Gemini V2.0, USA). The microstructure and morphology of samples were investigated with a TEM-100X electron microscope (TEM, Japan) operated at 100 kV. The morphology of samples was also examined under field emission scanning electron microscope (FESEM, Hitachi S-550) operated at 30 kV.

3 Results and discussion

3.1 XRD analysis

XRD patterns of the samples obtained at 80 and 700°C were shown in Fig. 1. All peaks correspond to the standard HAp diffraction pattern (JCPDS card No. 09–0432, Fig. 1c), and show no other phases. This indicated that the product we synthesized is pure HAp crystals. In Fig. 1a, the broad peak width of the diffraction pattern could be attributed to small crystal size. As seen in Fig. 1b, the (002) peak have higher peak intensity and more narrow width compared to Fig. 1a, it might be due to the high crystalline quality of HAp crystals grown after calcination at 700°C.

3.2 FTIR analysis

Figure 2 shows FTIR spectra of yeast cells (Fig. 2a), the sample obtained at 80°C (Fig. 2b) and 700°C (Fig. 3c), respectively. In Fig. 3a, the bands at 1421 cm^{-1} can be ascribed to C–H bending, the bands at 2927 cm^{-1} can be ascribed to C–H stretching vibration, at 1650 cm^{-1} to C=O, which are correspond to the yeast cells [19]. The bands at 563, 603 cm^{-1} were derived from the v_4 bending vibrations of P–O mode and the 873 cm^{-1} band resulted from the v_1 symmetric P–O stretching vibration [20]. The strong band at 1035 cm^{-1} was also assigned to the P–O stretching vibration of PO_4^{3-} [21]. The broad band at

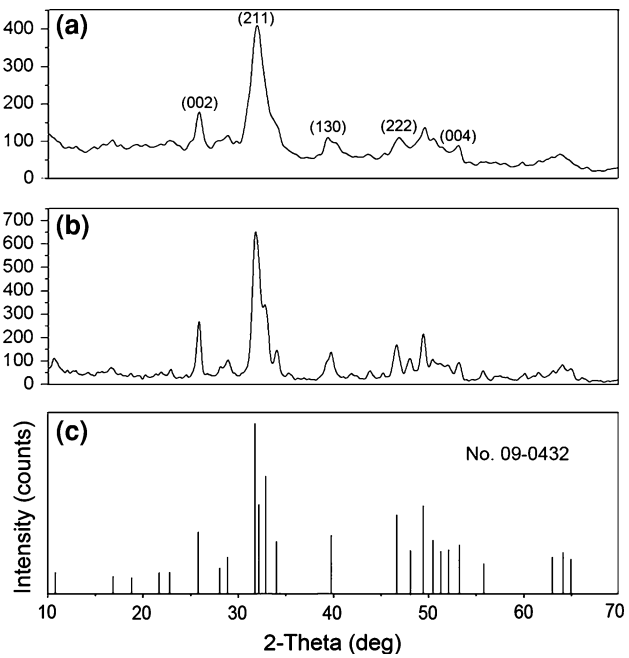

Fig. 1 XRD patterns of the samples **a** 80°C, **b** 700°C and (**c**) the standard HAp diffraction pattern (JCPDS, 09–0432)

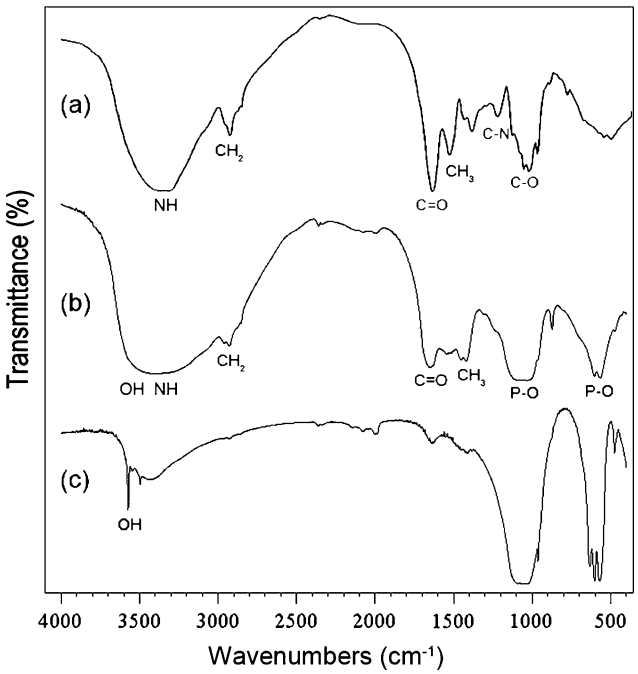

Fig. 2 FTIR spectra of (*a*) yeast cells and (*b*, *c*) the samples obtained at 80 and 700°C

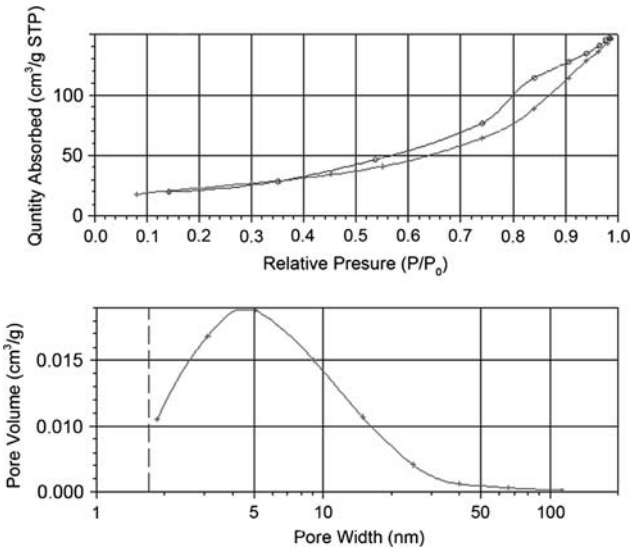

Fig. 3 N_2 adsorption/desorption isotherms and BJH pore size distribution of the HAp with yeast cells

3100–3500 cm^{-1} corresponds to adsorbed water, while the peak at 3571 cm^{-1} (Fig. 3c) corresponds to the stretching vibration of OH^- ions in the HA lattice [22]. The FTIR results indicated that microbial cells constituents were incorporated in the specimen. This indicated that the quality of the sample was excellent and only microbial cells constituents existed.

3.3 NADI and BJH anlysis

In Fig. 3, NADI of the sample obtained at 80°C shows the type IV isotherm behavior with a H_3-type hysteresis loop at a high relative pressure, it can be indicated that the sample have an inhomogeneous slit-shaped channel. The BET surface area of the sample is 86 m^2 g^{-1}, and the pore size distribution plot computed on the basis of BJH analysis indicate a distribution within the range of 2.0–40 nm and

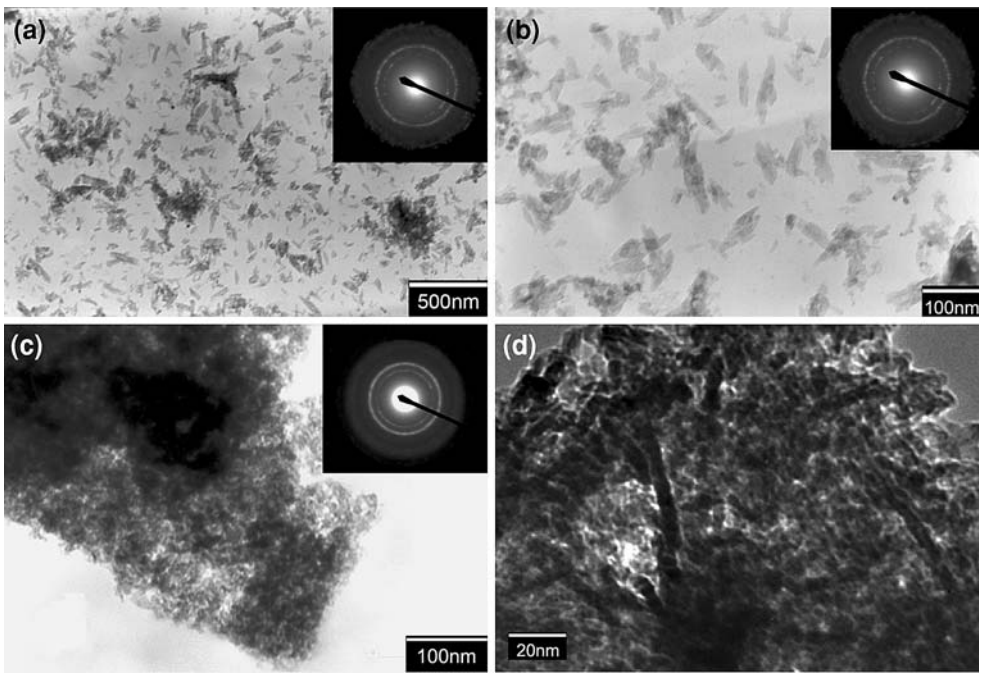

Fig. 4 TEM micrographs and electron diffraction patterns (inset) of the samples: **a** and **b** blank HAp, **c** and **d** HAp with yeast cells

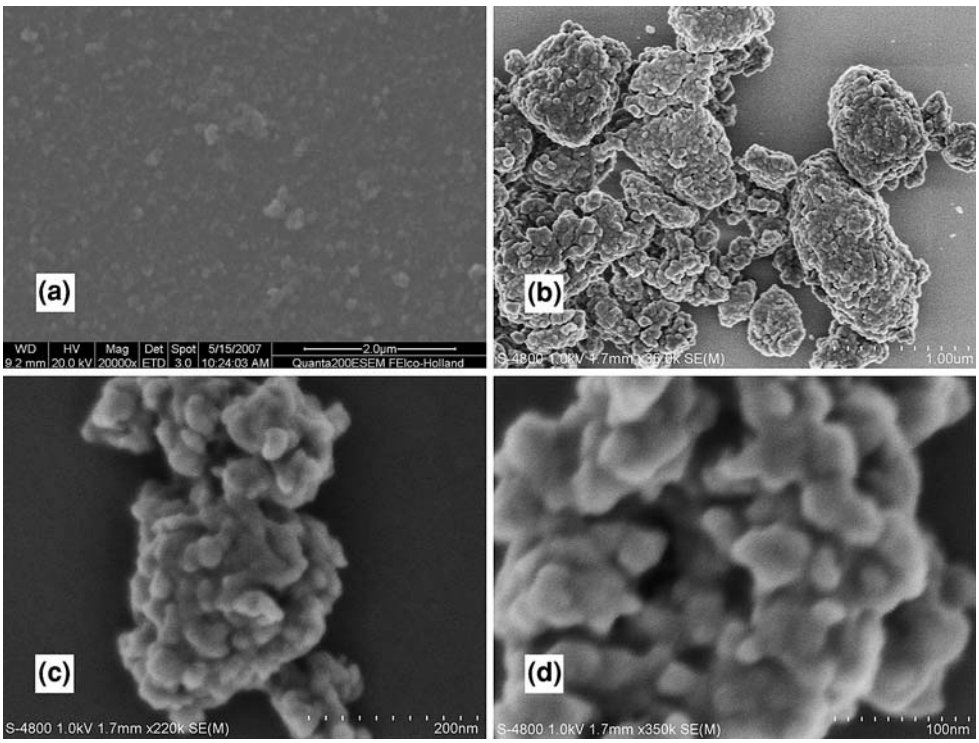

Fig. 5 FESEM micrographs of the samples: **a** blank HAp, **b–d** HAp with yeast cells at different magnifications

the maximum centered around 4.5 nm, reflecting a multi-pore texture of the sample.

3.4 TEM and FESEM analysis

Figure 4 shows TEM micrographs of the HAp samples both obtained at 80°C. In Fig. 4a and b, the blank HAp particles synthesized without any template, can be observed to be a bamboo leaf-shaped nanostructure, even though there is some agglomeration to some extent. In Fig. 4c, we can see the HAp with yeast cells is approximately hundreds of nanometer, and the particles are piled up by nano-grain with the diameter of 10–20 nm. It can be indicated that the addition of yeast cells can change the shape and size of sample. High-resolution TEM studies further confirm the existence of microbial cells constituents (Fig. 4d). In the electron diffraction pattern (inset of Fig. 4a and c), some diffraction rings can be seen. The crystal structure of these particles measured is hydroxyapatite style.

In Fig. 5, FESEM micrographs further support that the samples with mesoporous morphologies, wherein some porosity was found, while no porosity was found in blank HAp sample. The results indicate that yeast cells as the template, which provides nucleation sites for target materials, induced the nucleation and growth of the HAp. Along with a molecular template for apatite formation, the bio-structure of the yeast cells may contribute to the homogeneous deposition of the HAp. In the first step, Ca^{2+} absorbed in the surface of yeast cells [18]; in the second step, as the addition of P precursor, the HAp began to nucleate and growth; in the end, the HAp turned to be a hundreds of nanometer particles due to the shape of yeast cells. The formation process of the HAp with yeast cells can be schematically illustrated in Fig. 6.

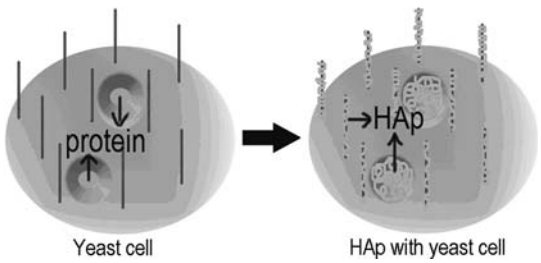

Fig. 6 The possible formation process of the HAp sample

4 Conclusions

Hydroxyapatite particles with mesoporous structure can be synthesized from the calcium hydroxide and di-ammonium hydrogen phosphate solution via a precipitation method, using yeast cells as the template. The size of HAp particles is approximately hundreds of nanometer. The pore width of HAp particles is in the range of 2.0–40 nm and the maximum centered around 4.5 nm. It shows that the yeast cells have great effects on the formation of mesoporous structured HAp particles.

Since the HAp particles exhibit a promising biological behaviour, they could be used in drug delivery agent and tissue engineering of bone. The further studies on this aspect will be carried out.

Acknowledgments This research was supported by the National Key Basic Research 973 Program of China (Grant 2005CB623902), National Natural Science Foundation of China (Grant 50572029) and Natural Science Foundation Team Project of Guangdong (Grant 04205786).

References

1. Temenoff JS, Mikos AG. Review: tissue engineering for regeneration of articular cartilage. Biomaterials. 2000;21:431–40.
2. Burg KJL, Porter S, Kellam JF. Biomaterial developments for bone tissue engineering. Biomaterials. 2000;21:2347–59.
3. Wang HN, Li YB, Zuo Y, Li JH, Ma SS, Cheng L. Biocompatibility and osteogenesis of biomimetic nano-hydroxyapatite/polyamide composite scaffolds for bone tissue engineering. Biomaterials. 2007;28:3338–48. doi:10.1016/j.biomaterials.2007.04.014.
4. Kokubo T, Kim HM, Kawashita M. Novel bioactive materials with different mechanical properties. Biomaterials. 2003;24:2161–75. doi:10.1016/S0142-9612(03)00044-9.
5. Dash AK, Cudworth GC. Therapeutic applications of implantable drug delivery systems. J Pharmacol Toxicol Methods. 1998;40:1–12.
6. Cheng WP, Gray AI, Tetley L, Hang TLB, Schätzlein AG, Uchegbu IF. Polyelectrolyte nanoparticles with high drug loading enhance the oral uptake of hydrophobic compounds. Biomacromolecules. 2006;7:1509–20. doi:10.1021/bm060130l.
7. Bezzi G, Celotti G, Landi E, La Torretta TMG, Sopyan I, Tampieri A. A novel sol–gel technique for hydroxyapatite preparation. Mater Chem Phys. 2003;78:816–24.
8. Andersson J, Areva S, Spliethoff B, Lindén M. Sol–gel synthesis of a multifunctional, hierarchically porous silica/apatite composite. Biomaterials. 2005;26:6827–35. doi:10.1016/j.biomaterials.2005.05.002.
9. Kumar R, Prakash KH, Cheang P, Khor KA. Temperature driven morphological changes of chemically precipitated hydroxyapatite nanoparticles. Langmuir. 2004;20:5196–200. doi:10.1021/la049304f.
10. Mobasherpour I, Soulati Heshajin M, Kazemzadeh A, Zakeri M. Synthesis of nanocrystalline hydroxyapatite by using precipitation method. J Alloys Compd. 2007;430:330–3. doi:10.1016/j.jallcom.2006.05.018.
11. Wang YJ, Zhang SH, Wei K, Zhao NR, Chen JD, Wang XD. Hydrothermal synthesis of hydroxyapatite nanopowders using cationic surfactant as a template. Mater Lett. 2006;60:1484–7. doi:10.1016/j.matlet.2005.11.053.
12. Bose S, Saha SK. Synthesis and characterization of hydroxyapatite nanopowders by emulsion technique. Chem Mater. 2003;15:4464–9. doi:10.1021/cm0303437.
13. Itatani K, Iwafune K, Scott Howell F, Aizawa M. Preparation of various calcium-phosphate powders by ultrasonic spray freeze-drying technique. Mater Res Bull. 2000;35:575–85.
14. Zarur AJ, Hwu HH, Ying JY. Reverse microemulsion-mediated synthesis and structural evolution of barium hexaaluminate nanoparticles. Langmuir. 2000;16:3042–9. doi:10.1021/la9908034.
15. Althues H, Kaskel S. Sulfated Zirconia nanoparticles synthesized in reverse microemulsions: preparation and catalytic properties. Langmuir. 2002;18:7428–35. doi:10.1021/la0202327.
16. Banat IM, Makkar RS, Cameotra SS. Potential commercial applications of microbial surfactants. Appl Microbiol Biotechnol. 2000;53:495–508.
17. Kitamoto D, Isoda H, Nakahara T. Functions and potential applications of glycolipid biosurfactants from energy-saving materials to gene delivery carriers. J Biosci Bioeng. 2002;94:187–201.
18. Breierova E, Vajczikova I, Sasinkova V, Stratilova E, Fišera M, Gregor T, Šajbidor J. Biosorption of cadmium ions by different yeast species. Z Naturforsch C. 2002;57:634–9.
19. Burattini E, Cavagna M, Dell'Anna R, Malvezzi Campeggi F, Monti F, Rossi F, et al. A FTIR microspectroscopy study of autolysis in cells of the wine yeast Saccharomyces cerevisiae. Vib Spectrosc. 2008;47:139–47.
20. Joris SJ, Amberg CH. The nature of deficiency in nonstoichiometric hydroxyapatites. II. Spectroscopic studies of calcium and strontium hydroxyapatites. J Phys Chem. 1971;75:3172–8.
21. Blakeslee KC, Condrate RA. Vibration spectra of hydrothermal prepared hydroxyapatites. J Am Ceram Soc. 1971;54:559–63.
22. Cheng ZH, Yasukawa A, Kandori K, Ishikawa T. FTIR Study on incorporation of into calcium hydroxyapatite CO_2. J Chem Soc Faraday Trans. 1998;94:1501–5.